[13] E. Feig and S. Winograd, "Fast algorithm for the discrete cosine transform," *IEEE Trans. Signal Processing*, vol. 40, pp. 2174–2193, Sept. 1992.

Design and Application of Discrete-Time Fractional Hilbert Transformer

Chien-Cheng Tseng and Soo-Chang Pei

***Abstract*—In this paper, the design problems and applications of the fractional Hilbert transformer (FHT) are investigated. First, the conventional Hilbert transformer is generalized to FHT. Its corresponding analytic signal is also defined to construct a single-sideband (SSB) signal for saving communication bandwidth. Then, several methods are presented to design finite and infinite impulse response FHTs including the Hilbert transformer-based method, all-pass filter-based method, optimization methods, etc. Next, we propose a secure SSB communication in which the fractional order of FHT is used as a secret key for demodulation. Finally, two-dimensional FHT is used to detect edges or corners of digital images.**

***Index Terms*—Filter design, Hilbert transformer.**

I. Introduction

Conventionally, the Hilbert transformer has been widely used in communication applications to generate single-sideband (SSB) signals by splitting the modulating signal into two components, which are 90° out of phase. This approach reduces the required bandwidth for transmission of the signal by half [1]. The Hilbert transform also has applications in the measurement of frequency deviations of rotating machines, investigation of the impulse response of systems, characterization of acoustical devices, etc. [2]. So far, several methods have been developed to design finite impulse response (FIR) and infinite impulse response (IIR) digital Hilbert transformers such as the Remez exchange algorithm [3], eigenfilter method [4], and weighted least squares method [5]. Moreover, there are several methods for implementing the Hilbert transformer, including switched-capacitor implementation [6], neural network [7], and multiplierless triangular array realization [8].

In 1996, Lohmann *et al.* [9] generalized the Hilbert transform by introducing two different definitions of what they called the fractional Hilbert transform. One definition is a modification of the spatial filter with a fractional parameter, and the other is based on the fractional Fourier transform. In [10], Pei and Yeh developed the discrete version of the fractional Hilbert transform and applied it to the edge detection of images. In [11], Zayed introduced another generalization of the Hilbert transform to obtain the signal's analytic part by suppressing the negative frequencies of the signal's fractional Fourier transform. So far, the research of fractional Hilbert transform is very young and needs to be explored. In this paper, the design problems and applications of the fractional Hilbert transformer (FHT) will be investigated.

Manuscript received August 1999. This paper was recommended by Associate Editor A. Skodras.

C.-C. Tseng is with the Department of Computer and Communication Engineering, National Kaohsiung First University of Science and Technology, Kaohsiung, Taiwan, R.O.C. (e-mail: tcc@ccms.nkfust.edu.tw).

S.-C. Pei is with the Department of Electrical Engineering, National Taiwan University, Taipei, Taiwan, R.O.C.

Publisher Item Identifier S 1057-7130(00)11662-3.

II. Digital Fractional Hilbert Transformer

A. Definition and Property

The ideal frequency response of an FHT with order ν is defined by

$$H_\nu(\omega) = \begin{cases} e^{-j\phi}, & 0 \le \omega < \pi \\ e^{j\phi}, & -\pi \le \omega < 0 \end{cases} \tag{1}$$

where $\phi = (\nu\pi/2)$. That is to say, a FHT is an ideal $(\nu\pi/2)$ phase shifter. We now describe three properties of the FHT.

1) FHT becomes the conventional Hilbert transformer (HT) when $\nu = 1$. $H_0(\omega) = 1$ when we choose $\nu = 0$. Thus, a signal passing through FHT with order $\nu = 0$ is unchanged.
2) It can be shown that $H_{\nu_1+\nu_2}(\omega) = H_{\nu_1}(\omega)H_{\nu_2}(\omega)$. This implies that the order additivity property is satisfied, i.e., a signal passes through the cascade systems of $H_{\nu_1}(\omega)$ and $H_{\nu_2}(\omega)$ and is equivalent to pass through the system $H_{\nu_1+\nu_2}(\omega)$.
3) The response $H_\nu(\omega)$ is periodic with ν. Since $H_{\nu+4}(\omega) = H_\nu(\omega)$ holds, the period of FHT is four.

Compute the inverse Fourier transform of $H_\nu(\omega)$. The corresponding impulse response is given by

$$h_\nu(n) = \begin{cases} \cos(\phi), & n = 0 \\ \sin(\phi)\dfrac{2\sin^2\left(\dfrac{n\pi}{2}\right)}{n\pi}, & n \ne 0. \end{cases} \tag{2}$$

It is clear that $h_\nu(n)$ becomes zero-valued when n is a nonzero even integer. Based on this result, the window method can be directly applied to design FIR FHT. After some maniputation, it can be shown that

$$h_\nu(n) = \cos(\phi)h_0(n) + \sin(\phi)h_1(n) \tag{3}$$

where $h_1(n)$ is the impulse response of the conventional HT and $h_0(n)$ is equal to unit sample function $\delta(n)$. Thus, FHT can be designed by slightly modifying the filter coefficients of conventional HT, which can be obtained by several well-documented methods. Taking the Fourier transform at both sides of (3), we obtain

$$H_\nu(\omega) = \cos(\phi)H_0(\omega) + \sin(\phi)H_1(\omega). \tag{4}$$

This means that the fractional Hilbert transform of a signal is a weighted sum of the original signal and its conventional Hilbert transform.

B. Single- Sideband Signal

Now, fractional HT is used to construct a single-sideband signal to save communication bandwidth. The details are described as follows. Given a real signal $x(n)$, its complex analytic signal $\hat{x}_\nu(n)$ is defined by

$$\hat{x}_\nu(n) = x(n) - e^{-j\phi}\overline{x}_\nu(n) \tag{5}$$

where $\overline{x}_\nu(n)$ is the output of the FHT with order ν by feeding signal $x(n)$. Taking the Fourier transform at both sides in (5), we have the expression in the frequency domain as

$$\hat{X}_\nu(\omega) = X(\omega) - e^{-j\phi}\overline{X}_\nu(\omega) \tag{6}$$

where $\overline{X}_\nu(\omega) = H_\nu(\omega)X(\omega)$. Substituting (1) into (6), we obtain

$$\hat{X}_\nu(\omega) = \begin{cases} 2je^{-j\phi}\sin(\phi)X(\omega), & 0 \le \omega < \pi \\ 0, & -\pi \le \omega < 0. \end{cases} \tag{7}$$

Thus, the negative frequency content of $\hat{x}_\nu(n)$ is all suppressed. When ϕ is not the multiple of π, i.e., $\sin(\phi) \ne 0$, the signal $\hat{x}_\nu(n)$ will contain the same information as $x(n)$ because both spectrums have a nonzero scale in the positive frequency domain. This elimination reduces the required bandwidth for processing and/or transmission of the signal by half. Finally, an example is used to demonstrate the above facts. If

$x(n)$ is a sinusoidal signal denoted by $\cos(\omega_0 n)$, its frequency-domain representation of fractional Hilbert transform is written as

$$\overline{X}_\nu(\omega) = \pi \sum_{k=-\infty}^{\infty} \left[e^{-j\phi}\delta(\omega - \omega_0 + 2\pi k) + e^{j\phi}\delta(\omega + \omega_0 + 2\pi k) \right]. \tag{8}$$

Taking the inverse Fourier transform, we obtain the time-domain representation as follows:

$$\overline{x}_\nu(n) = \cos(\omega_0 n - \phi). \tag{9}$$

Combine the above results. The analytic signal $\hat{x}_\nu(n)$ is given by

$$\hat{x}_\nu(n) = \cos(\omega_0 n) - e^{-j\phi}\cos(\omega_0 n - \phi) = je^{-j\phi}\sin(\phi)e^{j\omega_0 n}. \tag{10}$$

When we choose $\phi = (\pi/2)$, this result is reduced to $\hat{x}_\nu(n) = e^{j\omega_0 n}$.

C. Two-Dimensional FHT

The ideal frequency response of two-dimensional (2-D) FHT with order (ν_x, ν_y) is defined by

$$\begin{aligned} H_{\nu_x,\nu_y}(\omega_1, \omega_2) &= H_{\nu_x}(\omega_1)H_{\nu_y}(\omega_2) \\ &= \begin{cases} e^{-j(\phi_x+\phi_y)}, & 0 \le \omega_1 < \pi \text{ and } 0 \le \omega_2 < \pi \\ e^{-j(\phi_x-\phi_y)}, & 0 \le \omega_1 < \pi \text{ and } -\pi \le \omega_2 < 0 \\ e^{-j(-\phi_x+\phi_y)}, & -\pi \le \omega_1 < 0 \text{ and } 0 \le \omega_2 < \pi \\ e^{j(\phi_x+\phi_y)}, & -\pi \le \omega_1 < 0 \text{ and } -\pi \le \omega_2 < 0 \end{cases} \end{aligned} \tag{11}$$

where $\phi_x = (\nu_x\pi/2)$ and $\phi_y = (\nu_y\pi/2)$. That is to say, a 2-D FHT is an ideal $(\nu_x\pi/2)$ phase shifter in x-direction and an ideal $(\nu_y\pi/2)$ phase shifter in y-direction. From (11), it can be seen that the desired response $H_{\nu_x,\nu_y}(\omega_1, \omega_2)$ is separable for frequencies ω_1 and ω_2. Thus, the design problem of 2-D FHT can be reduced to two one-dimensional FHT design problems, i.e., design filter $G_1(z_1)$ to approximate response $H_{\nu_x}(\omega_1)$ and design filter $G_2(z_2)$ to fit response $H_{\nu_y}(\omega_2)$. As a result, 2-D filter $G_1(z_1)G_2(z_2)$ will approximate $H_{\nu_x,\nu_y}(\omega_1, \omega_2)$ very well. Finally, it is worth mentioning that multidimensional FHT can be also defined using separability like multidimensional HT described in [1, ch. 9].

III. Design of Fractional Hilbert Transformer

In this section, the design problem of the FHT is investigated. Because practical digital filters will introduce a delay and $H_\nu(\omega)$ in (1) is a zero delay specification, the FIR and IIR filters cannot be used to approximate the ideal response $H_\nu(\omega)$. To solve this problem, we let digital filters approximate the modified specification $F_d(\omega)$, which is the frequency response by cascading ideal FHT and a pure delay system, i.e.,

$$\begin{aligned} F_d(\omega) &= H_\nu(\omega)e^{-jn_0\omega} \\ &= \begin{cases} e^{-jn_0\omega}e^{-j\phi} & 0 \le \omega < \pi \\ e^{-jn_0\omega}e^{j\phi} & -\pi \le \omega < 0 \end{cases} \end{aligned} \tag{12}$$

where n_0 is a prescribed delay. Once an FIR or IIR filter $G(z)$ is designed, we use the following formula to obtain the designed result $\hat{H}_\nu(\omega)$ of the FHT:

$$\hat{H}_\nu(\omega) = G(e^{j\omega})e^{jn_0\omega}. \tag{13}$$

Moreover, when a signal passes through filter $G(z)$, it is equivalent to passing through a cascade system of a pure delay filter z^{-n_0} and a designed FHT with frequency response $H_\nu(\omega)$.

A. Design Based on Conventional Hilbert Transformers

From (4), we see that the FHT can be obtained from the designed result of conventional Hilbert transformer. The main result can be summarized as follows.

Fact 1: Let $D(\omega) = \cos(\phi)e^{-jn_0\omega} + \sin(\phi)e^{-jn_0\omega}H(\omega)$, where $H(w)$ is the ideal frequency response of conventional Hilbert transformer. Then it can be shown that

$$D(\omega) = \begin{cases} e^{-jn_0\omega}e^{-j\phi}, & 0 \le \omega < \pi \\ e^{-jn_0\omega}e^{j\phi}, & -\pi \le \omega < 0 \end{cases} \tag{14}$$

that is, $D(\omega) = e^{-jn_0\omega}H_\nu(\omega)$.

Based on this fact, two steps to design FHT from the conventional HT are as follows.

1) Design FIR or IIR Hilbert transformers $F(z)$ to approximate the desired frequency response $e^{-jn_0\omega}H(\omega)$ by using the well-documented methods.
2) The FHT $G(z)$ is given by $\cos(\phi)z^{-n_0} + \sin(\phi)F(z)$.

Note that filters $F(z)$ and $G(z)$ both have same filter length in the FIR filter case. Now, two examples are used to illustrate this design method. In the first example, we consider the design of IIR FHT. The parameters chosen are delay $n_0 = 11$ and $\nu = 0.4$. The IIR Hilbert transformer $F(z)$ with order 12/12, delay 11, and "care" band $[0.08\pi, 0.92\pi]$ is designed by the method proposed in [2]. The designed result of $F(z)$ has been shown in [2, Fig. 5]. Let $F(z)$ be denoted by $(B(z)/A(z))$. Then the FHT $G(z)$ is constructed by

$$\begin{aligned} G(z) &= \cos(\phi)z^{-n_0} + \sin(\phi)F(z) \\ &= \frac{\cos(\phi)z^{-n_0}A(z) + \sin(\phi)B(z)}{A(z)}. \end{aligned} \tag{15}$$

Because $F(z)$ and $G(z)$ have the same denominator polynomial $A(z)$, the filter $G(z)$ is stable if the filter $F(z)$ is stable. The design results $G(e^{j\omega})e^{jn_0\omega}$ are shown in Fig. 1(a) and (b). It is clear that the amplitude response approximates unit gain and the phase response -0.2π fits very well for all frequencies in the "care" band $[0.08\pi, 0.92\pi]$.

In the second example, we consider the design of FIR FHT. The parameters chosen are delay $n_0 = 20$ and $\nu = 0.4$. The McClellan–Parks algorithm with order 40 and cut frequencies $[0.03\pi, 0.97\pi]$ is first used to design Hilbert transformer $F(z)$. Then, the FHT $G(z)$ is constructed by $\cos(\phi)z^{-n_0} + \sin(\phi)F(z)$. The designed results $G(e^{j\omega})e^{jn_0\omega}$ are shown in Fig. 1(c) and (d). It is clear that the amplitude response approximates unit gain and the phase response fits -0.2π well for all frequencies except edge frequencies $\omega = 0$ and $\omega = \pi$.

B. Other Design Methods

Two other methods can be used to design FHT.

1) All-Pass Filter Approach: From (12), it can be seen that the amplitude response of $F_d(\omega)$ is equal to unity for all frequencies. The response can be approximated by the all-pass filter

$$G(z) = \frac{a_N + a_{N-1}z^{-1} + \cdots + a_1 z^{-N+1} + z^{-N}}{1 + a_1 z^{-1} + \cdots + a_{N-1}z^{-N+1} + a_N z^{-N}}. \tag{16}$$

Let the phase response of all-pass filter $G(z)$ be denoted by $\theta_G(\omega)$. Then our purpose is to design the all-pass filter $G(z)$ such that the $\theta_G(\omega)$ approximates the prescribed phase response $-n_0\omega - \phi$. Using the design method described in [12], the optimal filter coefficients $a_1, \ldots, a_N$ can be determined in the least squares error sense.

2) Optimization Method: The desired frequency response of the FHT has been specified in (12). Any general filter design methods that approximate a given magnitude and phase responses simultaneously can be applied to design a FHT. For example, we can use the quadratic programming approaches described in [13] to design optimal IIR FHT.

IV. Applications of Fractional Hilbert Transformer

In this section, we first use the FHT to construct a secure SSB communication system. The fractional number ν will be a secret key for demodulation. Then, 2-D FHT is applied to detect the locations of edges and corners in digital images.

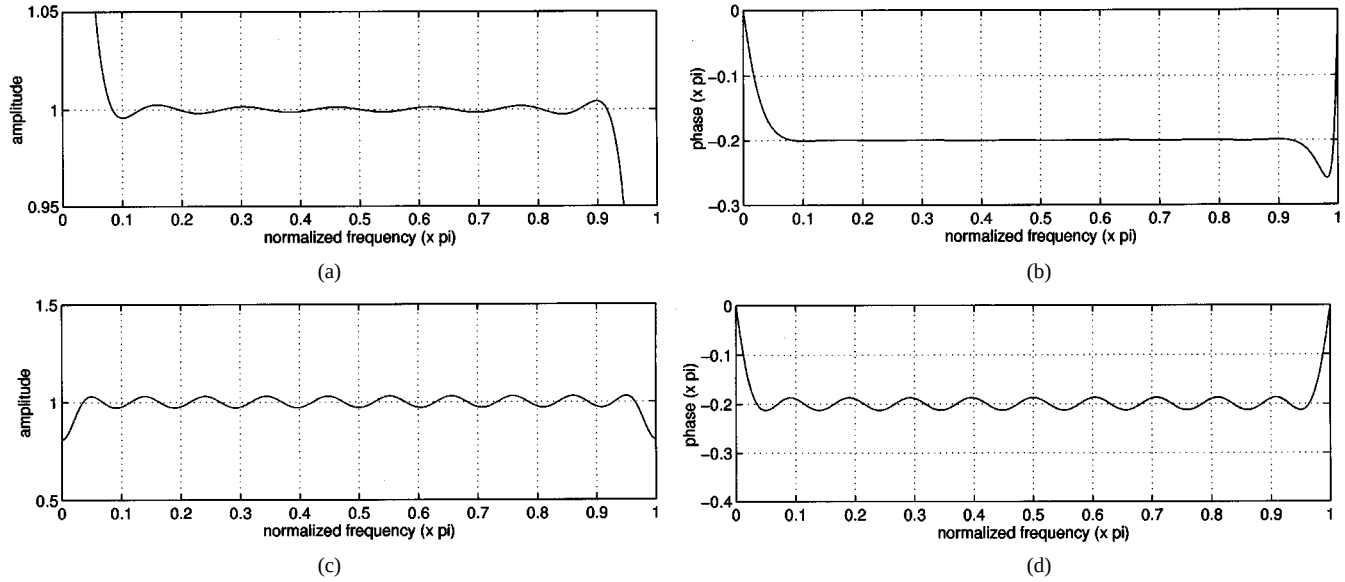

Fig. 1. (a) The amplitude response of the FHT designed by IIR HT. (b) The phase response of the FHT designed by IIR HT. (c) The amplitude response of the designed FIR FHT. (d) The phase response of the designed FIR FHT.

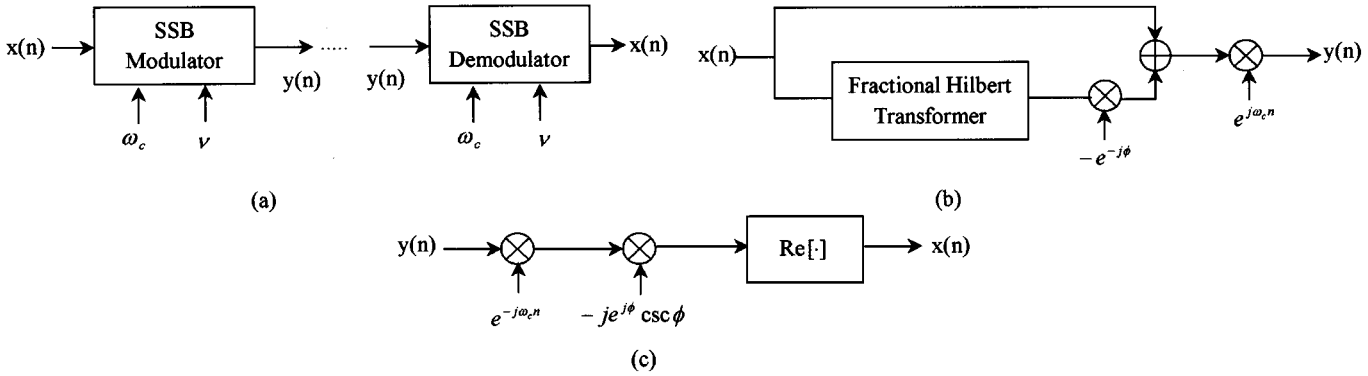

Fig. 2. (a) Secure SSB communication system. (b) The block diagram of the modulator. (c) The block diagram of the demodulator.

A. Secure SSB Communication System

The definitions of FHT and analytic signal have been stated in Section II. Now, we will use them to construct a secure SSB communication system shown in Fig. 2(a). ω_c is the carrier frequency and $\phi = (\nu\pi/2)$ is the fractional order of FHT. In this system, the order ϕ is used as a secret key for demodulation. If the order ϕ is unknown in the demodulation, the signal $x(n)$ will not be recovered from the received signal $y(n)$. Based on the definition of the analytic signal in (5), the block diagram of modulation is shown in Fig. 2(b). This process involves two steps. First, an analytic version of a real signal $x(n)$ is generated. Second, it is used to modulate a sinusoidal carrier of frequency ω_c. The spectrum $Y(\omega)$ of the complex modulated signal $y(n)$ is given by

$$Y(\omega) = \hat{X}_\nu(\omega - \omega_c) \tag{17}$$

where $\hat{X}_\nu(\omega)$ is described in (7). Moreover, we introduce the following fact to build the demodulation scheme.

Fact 2: Let the signal $s(n)$ be defined as

$$s(n) = -je^{j\phi}\csc(\phi)\hat{x}_\nu(n) \tag{18}$$

where $\hat{x}_\nu(n)$ is the analytic signal defined in (5). Then it can be shown that the real part of the signal $s(n)$ is $x(n)$, i.e.,

$$x(n) = \mathrm{Re}(s(n)). \tag{19}$$

Proof: Substituting (5) into (18), we have

$$s(n) = x(n) - j\ \cot(\phi)x(n) + j\csc(\phi)\overline{x}_\nu(n). \tag{20}$$

Since $x(n)$ and $\overline{x}_\nu(n)$ are both real signals, the real part of the signal $s(n)$ is $x(n)$.

Based on the above fact, the block diagram of demodulation is shown in Fig. 2(c). This process involves two steps.

1) The analytic signal is recovered by multiplying $y(n)$ with a sinusoid whose frequency is $-\omega_c$.
2) Use Fact 2 to obtain the signal $x(n)$ from its analytic version. In this demodulation scheme, it is clear that the parameter ϕ must be known in advance. Thus, parameter ϕ can be used as a secret key for demodulation.

Now, let us investigate two interesting problems. First, what is the output of demodulator if parameter ϕ in the demodulator is replaced by any parameter θ? In this case, it can be shown that the output of demoulator becomes $x(n)+I(n)$, where interference $I(n)$ is given by

$$I(n) = \frac{\sin(\theta-\phi)}{\sin(\theta)}\,\overline{x}_\nu(n). \tag{21}$$

If parameter θ is equal to ϕ, the interference becomes zero-valued. Otherwise, the output of demodulator is the desired signal $x(n)$ additive with an interference $I(n)$. Thus, illegal users can not demodulate the received signal $y(n)$ if order ϕ is unknown.

Second, what is the output of demodulator if its input $y(n)$ is corrupted by an additive noise $v(n)$? In this case, it can be shown that the

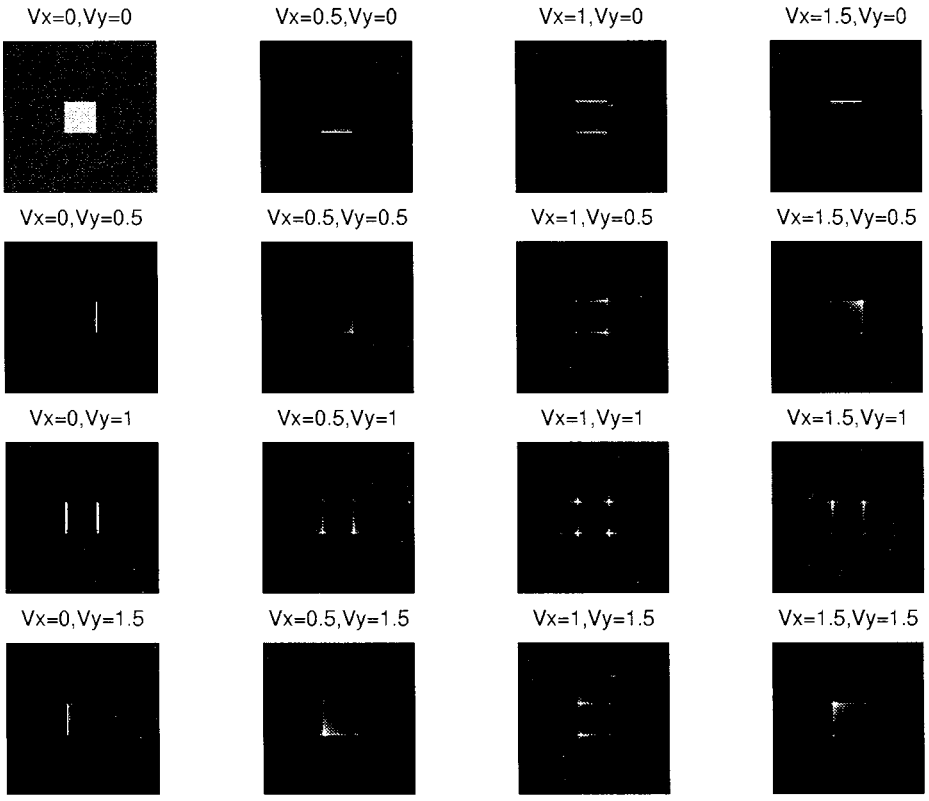

Fig. 3. The outputs of the 2-D FHT for various orders ν_x and ν_y. The input is an image corrupted by white noise.

output of demoulator becomes $x(n)+u(n)$, where noise $u(n)$ is given by

$$u(n) = \csc(\phi)\mathrm{Re}(-je^{j\phi}e^{j\omega n}v(n)). \tag{22}$$

If parameter ϕ approaches zero, $\csc(\phi)$ approaches infinity, i.e., noise $u(n)$ is very large. However, when ϕ is in the interval $[(\pi/6),\ (\pi/2)]$, then csc(ϕ) ranges from one to two. Thus, it had better to choose the screte key ϕ in the range $[(\pi/6),\ (\pi/2)]$ such that noise gain csc(ϕ) is very small.

B. Edge and Corner Detections

The main application of 2-D FHT is to detect the locations of edges or corners of digital images. Now, an example is used to illustrate this application. When an image $x(m,\ n)$ passes through the 2-D FHT, its output can be computed by the inverse Fourier transform of $\hat{X}(\omega_1,\ \omega_2)$ given by

$$\hat{X}(\omega_1,\ \omega_2) = H_{\nu_x,\ \nu_y}(\omega_1,\ \omega_2)X(\omega_1,\ \omega_2) \tag{23}$$

where $X(\omega_1,\ \omega_2)$ is the 2-D Fourier transform of $x(m,\ n)$ and $H_{\nu_x,\ \nu_y}(\omega_1,\ \omega_2)$ is 2-D FHT defined in (11). In the following, we will compute the 2-D fractional Hilbert transform of the 150×150 noisy image $x(m,\ n) = f(m,\ n) + v(m,\ n)$, where

$$f(m,\ n) = \begin{cases} 220, & 60 \le m \le 90 \text{ and } 60 \le n \le 90 \\ 0, & \text{otherwise} \end{cases} \tag{24}$$

and $v(m,\ n)$ is white Gaussian noise with standard deviation 20. Fig. 3 shows the results for various orders ν_x and ν_y. For clarity, all images have been displayed by properly thresholding. It is clear that the edges or corners in the image can be detected by suitably choosing the parameters ν_x and ν_y. Seven observations are listed as follows.

1) When $\nu_x = 0.5$ and $\nu_y = 0$, the horizontal negative derivative edges are emphasized.
2) When $\nu_x = 1$ and $\nu_y = 0$, the horizontal positive and negative derivative edges are both emphasized.
3) When $\nu_x = 1.5$ and $\nu_y = 0$, the horizontal positive derivative edges are emphasized.
4) When $\nu_x = 0$ and $\nu_y = 0.5$, the vertical negative derivative edges are emphasized.
5) When $\nu_x = 0$ and $\nu_y = 1$, the vertical positive and negative derivative edges are both emphasized.
6) When $\nu_x = 0$ and $\nu_y = 1.5$, the vertical positive derivative edges are emphasized.
7) When $\nu_x = 1$ and $\nu_y = 1$, four corner points are greatly emphasized.

The above observations tell us that the 2-D FHT provides more ways to detect edges or corners of digital images than the conventional Hilbert transform [14].

V. Conclusion

In this paper, the design problems and applications of the FHT have been investigated. However, only two applications are studied here, Thus, it will be interesting to apply FHT to other signal-processing applications in the future.

References

[1] S. L. Hahn, *Hilbert Transforms in Signal Processing*. Norwood, MA: Artech House, 1996.
[2] I. Kollar, R. Pintelon, and J. Schoukens, "Optimal FIR and IIR Hilbert transformer design via LS and minimax fitting," *IEEE Trans. Instrum. Meas.*, vol. 39, pp. 847–852, Dec. 1990.
[3] J. H. McClellan, T. W. Parks, and L. R. Rabiner, "A computer program for designing optimum FIR linear phase digital filters," *IEEE Trans. Audio Electroacoust.*, vol. AE-21, pp. 506–526, Dec. 1973.
[4] S. C. Pei and J. J. Shyu, "Design of FIR Hilbert transformers and differentiators by eigenfilter," *IEEE Trans. Circuits Syst.*, vol. 35, pp. 1457–1461, Nov. 1988.

[5] S. Sunder and V. Ramachandran, "Design of equiripple nonrecursive digital differentiators and Hilbert transformers using weighted least-squares technique," *IEEE Trans. Signal Processing*, pp. 2504–2509, Sept. 1994.
[6] K. P. Pun, J. E. Franca, and C. A. Leme, "Polyphase SC IIR Hilbert transformer," *Electron. Lett.*, vol. 35, pp. 689–690, Apr. 1999.
[7] A. Hiroi, K. Endo, H. Kamata, and Y. Ishida, "Design and implementation of an ideal Hilbert transformer using neural networks," in *Proc. IEEE Pacific Rim Conf. Communication, Computer and Signal Processing*, vol. I, 1993, pp. 292–295.
[8] S. Samadi, Y. Igarashi, and H. Iwakura, "Design and multiplierless realization of maximally flat FIR digital Hilbert transformers," *IEEE Trans. Signal Processing*, vol. 47, pp. 1946–1953, July 1999.
[9] A. W. Lohmann, D. Mendlovic, and Z. Zalevsky, "Fractional Hilbert transform," *Opt. Lett.*, vol. 21, pp. 281–283, Feb. 1996.
[10] S. C. Pei and M. H. Yeh, "Discrete fractional Hilbert transform," in *Proc. IEEE Int. Symp. Circuits and Systems*, vol. 4, May 1998, pp. 506–509.
[11] A. I. Zayed, "Hilbert transform associated with the fractional Fourier transform," *IEEE Signal Processing Lett.*, vol. 5, pp. 206–208, Aug. 1998.
[12] M. Lang and T. I. Laakso, "Simple and robust method for the design of allpass filters using least squares phase error criterion," *IEEE Trans. Circuits Syst. II*, vol. 41, pp. 40–48, Jan. 1994.
[13] W. S. Lu, S. C. Pei, and C. C. Tseng, "A weighted least-squares method for the design of stable 1-D and 2-D IIR digital filters," *IEEE Trans. Signal Processing*, vol. 46, pp. 1–10, Jan. 1998.
[14] K. Kohlmann, "Corner detection in natural images based on the 2-D Hilbert transform," *Signal Processing*, pp. 225–234, 1996.

Roundoff Noise Minimization in a Modified Direct-Form Delta Operator IIR Structure

Ngai Wong and Tung-Sang Ng

***Abstract*—Among various direct-form delta operator realized filter structures, the delta transposed direct-form II (δDFIIt) has been shown to produce the lowest roundoff noise gain in finite wordlength implementations. Recent analyses focus on the optimization of the free parameter Δ of the delta operator, with scaling of the structure to prevent arithmetic overflow. This paper proposes a modified δDFIIt second-order section in which the Δs and filter coefficients at different branches are separately scaled to achieve improved roundoff noise gain minimization. Expressions for the filter coefficients are derived, and reduction of roundoff noise gain is verified by numerical examples.**

***Index Terms*—Delta operator, IIR filter, minimization, roundoff noise.**

I. Introduction

Delta operator realized filters have attracted increasing attention in this decade due to their good numerical properties when compared to the traditional delay structures [1]–[8]. This is especially true for systems whose sampling rate is much higher than the underlying signal bandwidth, causing the z-plane poles to cluster toward the unit circle. By replacing the conventional z^{-1} operator with the inverse delta operator $\delta^{-1} = \Delta z^{-1}/(1 - z^{-1})$, certain ill-conditioned numerical issues in delay structures can be overcome. In particular, delta operator realizations are generally accompanied with better roundoff noise performance and more robust coefficient and frequency sensitivities [1], [2]. Although the inverse delta operator is more complicated to implement, its excellent numerical properties allow the use of shorter wordlengths, which results in moderate complexity or even gross savings in silicon area [6].

Manuscript received December 1999; revised October 2000. This work was supported by the Hong Kong Research Grants Council and by the University Research Committee of The University of Hong Kong. This paper was recommended by Associate Editor T. Stathaki.

The authors are with Department of Electrical and Electronic Engineering, The University of Hong Kong, Hong Kong (e-mail: nwong@eee.hku.hk; tsng@eee.hku.hk).

Publisher Item Identifier S 1057-7130(00)11663-5.

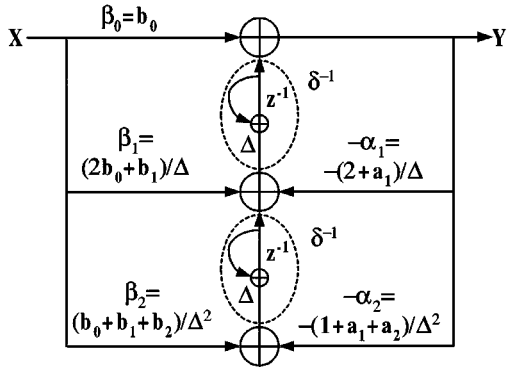

Fig. 1. Delta equivalence of delay structure with transfer function given by (1).

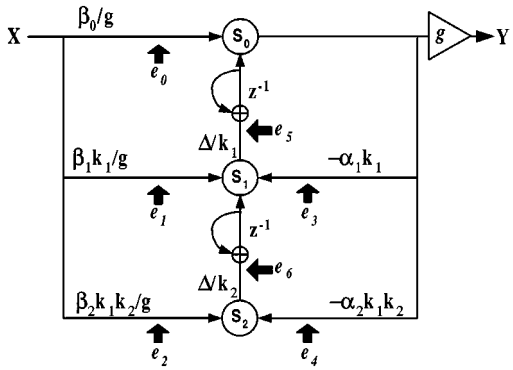

Fig. 2. Modified delta section with overflow scaling by g, and Δ and coefficient scaling by k_1 and k_2.

Comprehensive study of different delta structures has been carried out in [4]. It was found that the delta transposed direct-form II (δDFIIt) shows the best roundoff noise properties among various delta structures. Emphasis has been put on the optimization of the free parameter $\Delta(\Delta > 0)$ of the delta operator in order to achieve minimum roundoff noise gain at the output. The second-order δDFIIt section, being a basic building block, was analyzed in detail [3], [4].

In this paper, instead of limiting to a single optimal Δ within the second-order δDFIIt section, the concept of separately scaling the Δs as well as filter coefficients is introduced. It will be shown that such an approach will enable the true global optimal solution to be obtained, which further minimizes the roundoff noise gain of the section.

II. Noise Minimization

Suppose that a transfer function in the z-domain, represented by (1), is obtained under certain specifications and sampling conditions. It can then be transformed into an equivalent delta structure with the substitution $z = 1 + \delta\Delta$. Fig. 1 shows the δDFIIt implementation of (1). This structure was studied extensively for optimization in previous works [3], [4], where the same Δ was used in both δ^{-1} operators. Fig. 2 shows